Internally circulating fluidized-bed reactor for syngas production using chemical looping reforming

Mogahid Osman, Abdelghafour Zaabout, Schalk Cloete, Shahriar Amini

PII: S1385-8947(18)31955-7
DOI: https://doi.org/10.1016/j.cej.2018.10.013
Reference: CEJ 20076

To appear in: *Chemical Engineering Journal*

Received Date: 20 June 2018
Revised Date: 30 August 2018
Accepted Date: 2 October 2018

Please cite this article as: M. Osman, A. Zaabout, S. Cloete, S. Amini, Internally circulating fluidized-bed reactor for syngas production using chemical looping reforming, *Chemical Engineering Journal* (2018), doi: https://doi.org/10.1016/j.cej.2018.10.013

Internally circulating fluidized-bed reactor for syngas production using chemical looping reforming

Mogahid Osman[1], Abdelghafour Zaabout[2], Schalk Cloete[2], Shahriar Amini[1,2*]
[1]Norwegian University of Science and Technology, [2]SINTEF Industry
Trondheim, Norway

Abstract

Chemical looping reforming (CLR) is a promising method for achieving autothermal methane reforming without the energy penalty of an air separation unit that is required for partial oxidation (POX) or oxygen-blown autothermal reforming (ATR). Scale-up of the conventional dual circulating fluidized bed CLR configuration is challenging, however, especially under the pressurized operating conditions required for high process efficiency. The internally circulating reactor (ICR) concept has previously been proposed as a simplified solution for chemical looping, especially under pressurized operation. It assembles the chemical looping process into a single reactor with two sections connected by specially designed ports for oxygen carrier circulation. This study has successfully demonstrated CLR operation in a dedicated ICR test unit with a NiO oxygen carrier. Up to 3 kW of methane feed was reformed to syngas, achieving conversion efficiencies as high as 98%. The reactor behaved largely as expected over a range of CH_4/O_2 ratios and in a case with steam addition. Autothermal reactor operation could also be achieved, illustrating the practicality of the ICR concept. Based on this positive first demonstration study, further study of the ICR concept is recommended.

Keywords: Chemical Looping Reforming; Internally Circulating Reactor; Syngas Production; Pressurized Fluidized-bed Reactor; Oxygen Carriers

*Corresponding author: Dr. Shahriar Amini, SINTEF Industry, S.P. Andersens vei 15 B, 7031, Trondheim, Norway, Phone: +47 46639721, Email: shahriar.amini@sintef.no

1. Introduction

Natural gas reforming to syngas is the main commercial process for the production of hydrogen, ammonia, methanol and other important chemicals [1]. Catalytic steam methane reforming (SMR) is the most widely used approach in industry for syngas production [2,3]. SMR reactions are highly endothermic and reaction heat is generally supplied by external combustion of a fossil fuel with air, leading to significant CO_2 emissions [2,3]. Other technologies for syngas production has also been applied in industry in the last decade, including partial oxidation (POX) and autothermal reforming (ATR) [4]. POX produces syngas by partially oxidizing a hydrocarbon fuel with pure oxygen in a catalytic or non-catalytic reactor vessel. The main advantages of POX are its ability to reform higher hydrocarbons and avoid the need for external combustion. However, a large quantity of pure oxygen is required, thus demanding substantial investment and energy costs to construct and operate an air separation unit (ASU). ATR is a combination of SMR and POX technologies, in which pure oxygen or air co-feed with natural gas and steam. The exothermic POX reaction provides the necessary heat for the endothermic reforming reactions. However, ATR requires an ASU to supply a high quality syngas (high fraction of CO and H_2). If air used directly, the product gas will be diluted with nitrogen, imposing additional costs and efficiency penalties unless nitrogen is required as in ammonia production.

Chemical looping reforming (CLR) has emerged as a promising technology for syngas production with the potential to address the key shortcomings mentioned above for the conventional techniques. CLR can achieve autothermal methane reforming without external combustion reaction or an ASU, and obtain a N_2 free syngas stream without an ASU [5,6]. Moreover, CLR reduces the energy penalty associated with an SMR plant with post-combustion

CO_2 capture. A techno-economical study of different natural gas reforming technologies has shown that CLR with CO_2 capture is the most financially attractive option with a CO_2 avoidance cost of only \$5/tonne CO_2 relative to conventional SMR. SMR and ATR with CO_2 capture need CO_2 prices more than \$100 and \$50/tonne CO_2, respectively, to be a feasible option [7]. The study also found that CLR without CO_2 capture can be cheaper than conventional SMR.

The typical CLR system involves circulation of an oxygen-carrier (a metal-oxide material) between two interconnected reactors, namely the air reactor and the fuel reactor [8]. The material acts as an oxygen and heat transfer medium as well as a catalyst [6,8,9]. In the fuel reactor, the fuel reacts with the metal oxide to form the reformer gas (a mixture of H_2, CO, H_2O and CO_2) where the reduced metal also acts as a catalyst and heat supply for the reforming reactions, (Fig. 1, shows a simplified scheme of the working principle of the CLR process). In the air reactor, the reduced metal is oxidized and heated by the highly exothermic reaction before being transferred to the fuel reactor for continuous cyclic operation. Steam or CO_2 could be introduced with the fuel to enhance the reforming reaction and control the desired H_2/CO ratio in the produced syngas. It should be mentioned though, that steam or CO_2 addition is not a requirement because the part of the fuel being combusted during the autothermal reforming process will directly supply H_2O and CO_2 in the fuel reactor.

The CLR concept have been demonstrated at atmospheric pressure in a laboratory and pilot plant scale up to 140 kW (while natural gas CLR is the most widely studied [6,8,10–12], also liquid and solid fuel have been used for syngas production [13–17]). The performance of CLR under pressurized conditions was studied by Ortiz et al. [9] in a semi-continuous fluidized-bed reactor. The effect of total pressure on the CLR process using methane as fuel and nickel based oxygen-carriers was investigated. The results showed high conversion of methane and no effect of increasing the pressure on the products distributions. Extensive review of the recent CLR operational experiences can be found elsewhere [18,19].

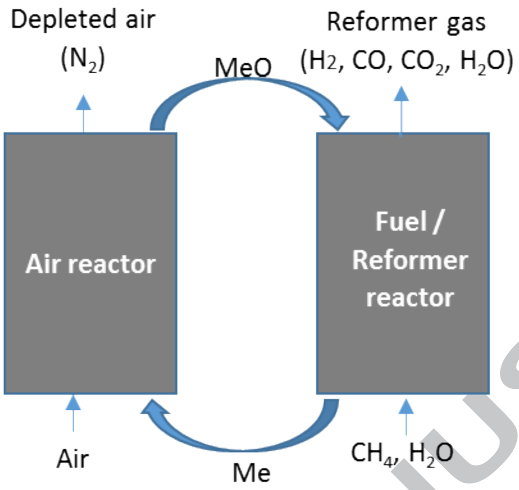

Fig. 1. Schematic diagram of the CLR process.

Pressurized operation of the CLR process is essential to maximize thermodynamic and economic performance. In the case of hydrogen production, pressurized operation minimizes the energy and capital cost related to hydrogen separation and compression. Syngas to liquids processes also require a pressurized syngas to maximize conversion efficiency. Furthermore, pressurized operation significantly reduces the plant footprint. A thermodynamic assessment has indeed shown that a 5% increase in energy efficiency could be achieved if CLR is operated under pressurized conditions, mainly gained from the energy saving made in H_2 and CO_2 compression [19]. The benefits of pressurized CLR operation addressed in the literature in various aspects including thermodynamic analysis, techno-economic studies, kinetic analysis and lab and pilot scale demonstration [9,19–21].

However, most experimental studies on chemical looping are based on operation at atmospheric pressure, as a circulating fluidized-bed reactor is the most widely studied reactor type for the CLR system. This configuration has been demonstrated experimentally at lab [5,6,12] and pilot scales [8]. To the best knowledge of the authors, only two studies have so far reported on pressurized interconnected fluidized beds for CLC. Wang et al. [22] carried out a pressurized CLC for coke-oven gas, where the operational pressure of the system was 3 bar and the maximum operating temperature was 950°C. More recently, Xiao et al. conducted solid fuel CLC at three pressure levels (1, 3 and 5 bar) [23]. The results showed that pressurized operation improved carbon conversion as well as CO_2 capture purity and combustion efficiency. However, higher losses of oxygen-carrier particles were reported with increasing pressure due to a decrease in the fuel reactor cyclone capture efficiency at elevated pressure. In this type of configuration, the system consists of two reactors, two loop seals and two cyclones to avoid gas leakage between the fuel and air reactors and achieve high gas-solid separation at the reactor outlets. Tightly controlled solids circulation between the two interconnected reactors, required to fulfill the heat and mass balance of the chemical looping process, presents a significant scale-up challenge, especially under pressurized conditions.

The need for pressurized CLR operation has inspired research into alternative reactor configurations that avoid external solids circulation. One such reactor configuration is the gas-switching concept, where the oxygen carrier material is stationary in one compact unit and exposed to alternate streams of air and fuel [24,25]. This arrangement greatly simplifies the reactor design and scale-up, but a coordinated cluster of reactors is required to achieve steady operation. The gas switching concept has been studied using packed-bed [25,26] and fluidized-bed configurations [27,28]. The packed bed system imposes several challenges including the requirement for pelletized oxygen-carrier materials, more pronounced carbon deposition, large thermo-chemical stresses on the oxygen carrier, and the requirement for reactor shutdown for replacement of the spent oxygen carrier material [29]. The fluidized bed configuration circumvents these material-related challenges but suffers moderate losses in process and CO_2 capture due to the good mixing taking place in the reactor [29]. The most important technical uncertainty related to the gas switching technology at present is the need for high temperature outlet valves [29]. CLR typically operates at lower temperatures than CLC, thus minimizing this challenge. Other reactor concepts proposed in the literature are the moving bed [30] and rotating reactor [31,32].

However, the steady-state nature and high gas throughput rates of the dual circulating fluidized-bed configuration remains attractive even when considering the challenges of pressurized operation. Simplifying the solids circulation mechanism for this reactor setup promises to accelerate scale-up and eventual commercialization. For this reason, this paper investigates the recently proposed internally circulating reactor (ICR) where the loop seals involved in the conventional configuration are replaced by simple ports between two sections in a single vessel [33], with a freeboard on the top replacing the cyclones. ICR can operate similarly to the interconnected configuration, where solids circulation between the two sections is achieved by feeding gasses into the two sections at different velocities. The high velocity gas feed in the fast section transports solids to the freeboard. The decelerated solids in the freeboard (due to the larger section area) fall into the upper port to circulate to the second section operating at low velocity (the slow section). Accumulation of solids in this section leads to static pressure building up, hence forcing the solids to circulate back to the fast section through the port at the bottom.

Combining the functionality of both reactors, cyclones and loop seals into a single unit is expected to simplify operation and design and reduce costs under pressurized conditions. The ICR unit can be designed as a single pressure vessel, whereas the conventional dual circulating fluidized bed configuration requires a separate pressure shell for each component. In addition, the short and simple ports will simplify control of the high solids circulation rates required under pressurized operation, relative to the much more elaborate system of cyclones, loop seals and relatively long solids transport lines connecting the reactors in the dual circulating fluidized bed configuration. Due to the simplified solids circulation mechanism, pressure imbalances between the reactors will be less likely and a wider range of operating conditions should be achievable.

The most important trade-off the ICR configuration is however, the gas leakage when using the simple ports instead of dedicated loop seals. A hydrodynamic investigation on a pseudo-2D cold-flow unit has revealed that a stable solids circulation and minimum gas leakage could be achieved with the ICR over a wide range of operating conditions [33]. This conclusion was confirmed by reactive multiphase flow modelling of a large-scale ICR unit (100 MWth) reactor [34]. Such a reactor configuration, based on internally circulating fluidized bed, was first proposed as an oil shale retort in 1986 [35] and was later widely used as a simplified version of the interconnected fluidized bed to evaluate the performance of different oxygen carrier materials under CLC and CLR process conditions on an atmospheric small lab scale [6,11,13,36–40].

In light of the promising results from the hydrodynamic study and the reactive simulations, the ICR unit shown in Fig. 2 has been constructed and commissioned to operate under fully reactive high temperature pressurized conditions. The aim of this study is to experimentally study the feasibility of the ICR concept for chemical looping reforming of methane, as well as to obtain insights about this type of reactor configuration in terms of ability of autothermal operation, achieving minimal leakage between the reactor sections and stable solids circulation under reactive conditions. This study represents the first demonstration of our proposed ICR concept under reactive conditions.

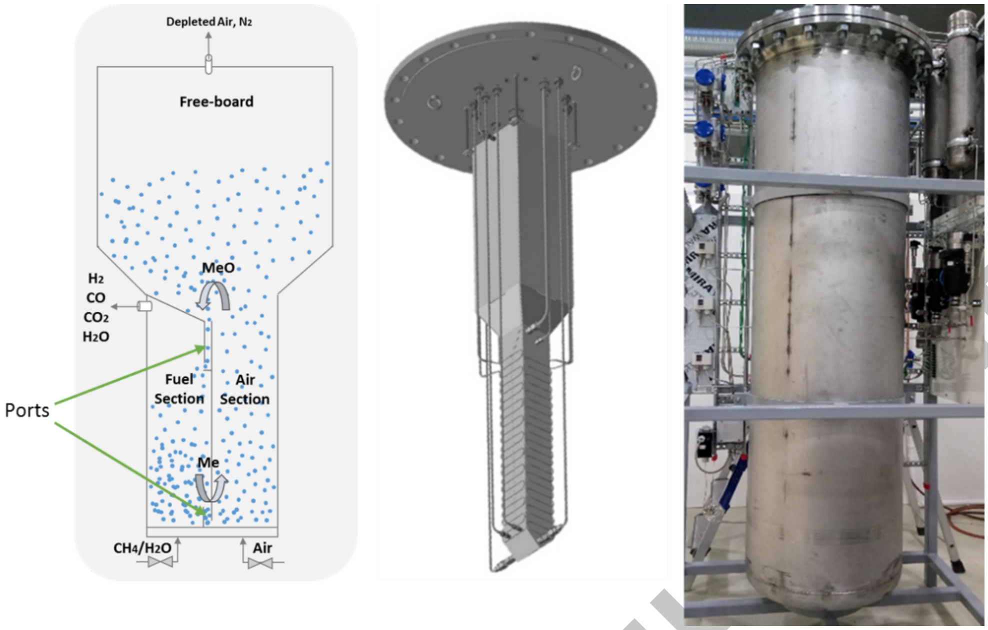

Fig. 2. Simplified scheme of the ICR design, CAD drawing of the ICR unit, and the ICR unit under operation inside the shell. .

2. Methodology

2.1. ICR unit

A lab scale ICR shown in Fig. 2. has been constructed and commissioned. The reactor was made of Inconel material (Inconel Alloy 625) to withstand high temperature conditions. It has a square section of 10 cm width and 70 cm height, divided into two sections (air reactor and fuel reactor) by a vertical partition, with connecting ports in between, at the top and the bottom, for solids circulation. An expanding freeboard region is added to the air reactor (AR) where the depleted air transporting oxygen carrier from the AR is decelerated to avoid particle elutriation, thereby allowing the oxygen carrier to fall into the upper port and circulates to the fuel reactor (FR). With this configuration, fast and bubbling fluidization regimes can be established in the air and fuel reactor respectively. The gas feed to each reactor section is completed using a perforated cylindrical tube at the bottom of each section. This relatively concentrated injection mechanism may reduce the quality of gas-solid contact in the lower regions of the reactor compared to a conventional porous plate but was selected due to substantial simplification offered in terms of reactor design and construction. The ports connecting the two sections are L-type connection ports, which were adopted instead of a simple orifice to create conditions with solids flowing close to maximum packing. Such a flow condition creates a physical plug that minimizes undesired gas leakage through the port.

The reactor was placed in a cylindrical shell designed to withstand pressures up to 12 bar. The reactor can be heated up to the target operating temperature using external electrical heaters surrounding the bottom part of the reactor body. Insulating material (glass wool) was placed around the reactor to minimize heat losses. The pressures inside the reactor and the shell were controlled using back-pressure regulators placed on the outlet of each reactor section and the shell. The reactor exhaust stream was cooled with a water cooler installed on the outlet of each section. A low temperature filter (40 μm pore size) was installed after the cooler to prevent fine particles elutriation to the environment. The feed flow rate to each section was controlled by Bronkhorst mass flow controllers. The dry gas composition (sampled after the back-pressure valve) was measured at 1 Hz frequency using a syngas analyzer type MCA 100 Syn-P from ETG Risorse e Tecnologia.

The experimental set up was equipped with different additional devices (DP cells, pressure sensors, thermocouple etc.) to monitor the reactor operation (solids circulation, temperature and pressure inside the reactor, etc., in addition to devices used for safety). Fig. 3 gives an overview of the reactor design and shell and the P&ID showing the different parts forming the set-up.

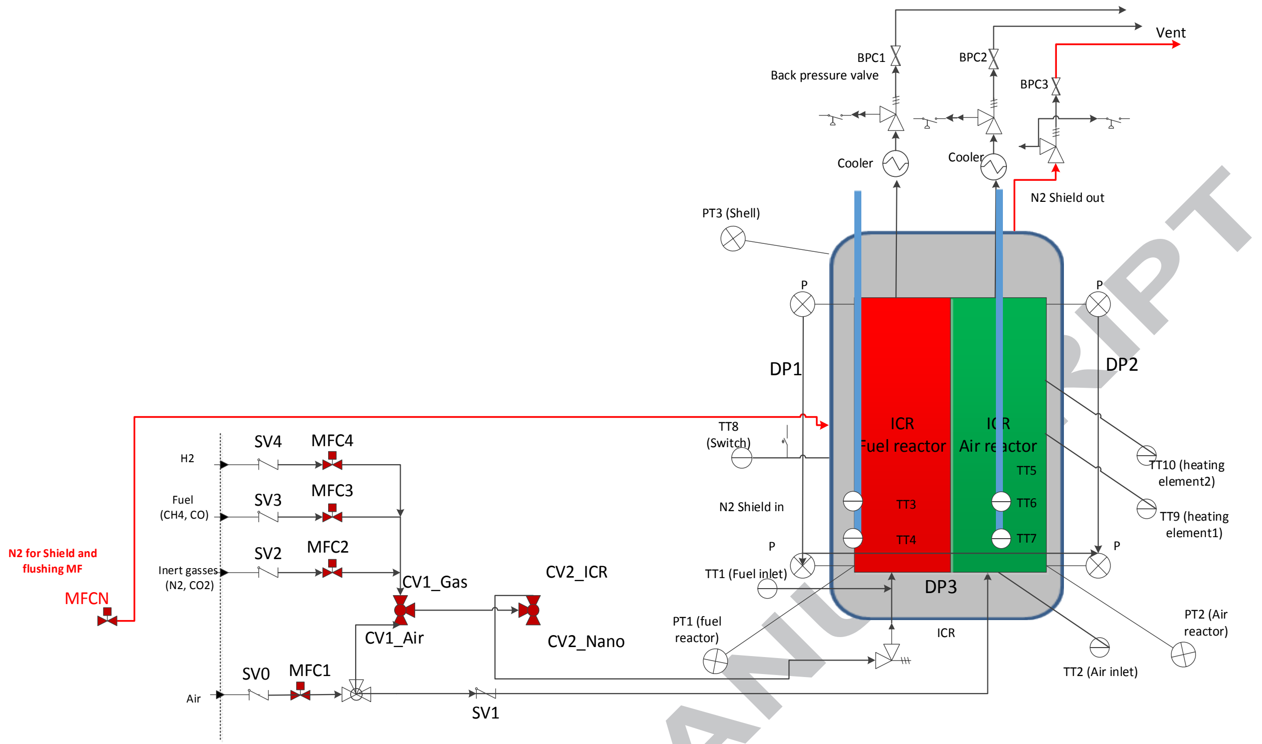

Fig. 3. P&ID diagram of the ICR unit.

2.2. Oxygen carrier

In this study, a highly active oxygen carrier manufactured by VITO, was used. The oxygen carrier is based on NiO particles supported on Al_2O_3; the NiO/Al_2O_3 ratio was 65/35, but resulted in around 37% free NiO (based on weight) sites which are available for reaction, while the rest reacted to $NiAl_2O_4$ during heat treatment used in the spray drying manufacturing process [41]. The particle size cut-offs D10, D50, and D90 were measured to be 117.4, 161.7 and 231.3 mm respectively. The oxygen carrier had a loosely packed density of 1950 kg/m^3 and a tapped density of 2166 kg/m^3. This oxygen carrier was selected because it has been successfully used in previous studies, and showed high reactivity and durability [42,43]. It should however be emphasized that the selection of an optimal oxygen carrier is out of the scope of this study; the main aim is to demonstrate the experimental feasibility of the ICR concept applied to CLR.

2.3. Fuel

Methane was used as fuel in most experiments, although CO was also used initially to verify that good solids circulation is achieved. Steam could be added with the fuel by a steam generator at a temperature of 200°C. The steam is fed to the reactor in a heated tube to prevent condensation. When desired, it was also possible to dilute the fuel with CO_2 or N_2.

2.4. Experimental procedure

The experience and knowledge gained from operation of a pseudo-2D cold unit built in our previous studies [33], were used to design a safe operating window of the ICR reactor. The link between solids circulation rate and the gas leakage between the two sections was quantified and understood in the pseudo 2D experiments. Similar methodology was followed in the constructed 3D reactor, operated under cold and hot (electrical heating) conditions with feeding of non-reactive gasses, to identify feed conditions that result in minimal gas leakage and steady solids circulation between the reactor sections. For all experiments, a total mass of 2 kg of NiO/Al_2O_3 particles was used (corresponding to 10 cm static bed-height). The reactor was electrically heated to 650 °C before feeding reactive gases. During the reactive experiments, the power of the heater was adjusted between 0 to 100% depending on the operating conditions. For autothermal operation, the heater power was set to 0%. Due to technical limitation, the set point temperature of the heating elements surrounding the reactor is limited to a maximum value of 820 °C. For this reason, all the experiments presented on this paper were carried out below this limit.

Before conducting the reactive experiments, initial tests were carried out to define an operating window in which solids circulation is achieved. The tests were completed by feeding a reactive gas, CO, to the fuel reactor (FR) and N_2 to the air reactor (AR), into a fully oxidized bed of oxygen carrier material. CO is highly reactive with NiO, and the CO breakthrough curves can therefore be used to clearly see whether circulation is transferring additional fully oxidized oxygen carrier from the AR to the FR under different gas feed rates to the air section. The outlet gas flowrates from each section were adjusted to be equal to the respective inlet gas flowrates by means of a manual needle valve placed on the outlet of the FR, while a rotameter was placed on the outlet of the AR. It should be noted that controlling flow rates at the outlets of the ICR sections affects the amounts of occurring gas leakage and solids circulation [33,34].

After defining operating conditions in which stable solids circulation is achieved, another set of experiments was conducted to quantify the gas leakage between the two ICR sections. This test was done by feeding CO_2 to FR and air to AR under external heating. CO_2 recovery and purity were calculated based on the amount of measured gas leakage from each section to the other.

In the CLR tests, seven experimental cases were considered in the current study. The main objective of the CLR process is to selectively produce syngas, which can be achieved by controlling various parameters in the system. The main operating variable is the CH_4/O_2 ratio in the FR, which can be altered by three parameters: solids circulation rate, oxygen feed to the AR and CH_4 feed to the FR. In all cases, the solids circulation was kept constant using constant fluidization velocities to both sections at a constant loading of the OC. At these conditions, bubbling and fast fluidization regimes in the FR and AR, respectively, were established. The fuel side fluidization velocity was estimated by assuming that methane will expand in volume by a factor of three after reacting to form syngas (with assuming full methane conversion).

Four cases were completed by changing CH_4 concentration in FR and two cases by changing O_2 concentration in AR for comparison. N_2 was used for dilution of the feed in both sections to maintain the total flow rate constant. One additional case was carried out with co-feeding steam with CH_4. A summary of the experimental cases is given in Table 1 and Table 2 . It should be noted that all experiments were carried out at 1.7 bara pressure and that the experimental results represent an average over at least 10 minutes of steady state operation. It is worth mentioning that approximately 3% of the total solids loading was lost as fines after all CLR operation. The lost fines were mainly recovered on the water trap in the heat exchanger after the FR and the on the filter after the AR. The ones collected on AR mainly originated from the fines in the fresh solids placed initially in the reactor before experiments, while the ones collected on FR contained larger particles that seem been elutriated from the bed, possibly due to sudden large bursts of gas that leaked from AR to FR.

Table 1. Summary of the experimental cases conducted in this study.

Experimental cases	Fuel-reactor (flowrate Nl/min)					Air-reactor (flowrate Nl/min)	
	CH_4	N_2	Steam	CO	CO_2	Air	N_2
Case-1	-	-	-	20	-	-	0, 70, 80, 90
Case-2	-	-	-	-	15	80	-
Case-3	3	6	-	-	-	80	-
Case-4	3.5	4.5	-	-	-	80	-
Case-5	4	3	-	-	-	80	-
Case-6	5	-	-	-	-	80	-
Case-7	4	3	-	-	-	25	55
Case-8	5	-	-	-	-	20	60
Case-9	4	-	3	-	-	80	-

Table 2. Summary of CLR operating conditions

Fuel	CH_4
Oxygen carrier	NiO/Al_2O_3
Particle size	~161.7 µm
Particle loading	2 kg (10 cm static bed-height)
Temperature	650 °C (initial temperature)
Pressure	1.7 bara
Flow rate in AR	80 Nl/min
Flow rate in FR	15 Nl/min

2.5. Data evaluation

Reactivity of fuel with OC particle are expressed by γ_{CH_4}, the carbon conversion of methane, which is defined as in Eq. (1):

$$\gamma_{CH_4} = \frac{x_{CO_2} + x_{CO}}{x_{CH_4} + x_{CO_2} + x_{CO}} \quad (1)$$

where x_i is the volume fraction of compound i in the dry gas leaving the FR.

In the non-reactive gas leakage experiments, CO_2 recovery was calculated as the ratio between the CO_2 leaking from the FR and the total amount of CO_2 in the FR (Eq. (2)). Similarly, CO_2 purity was calculated as the ratio between the air leaking from the AR and the total amount of CO_2 in the FR (Eq. (3)):

$$\mathrm{CO_2\ recovery} = \left(1 - \frac{\mathrm{CO_2\ flowrate\ at\ AR\ outlet}}{\mathrm{CO_2\ flowrate\ at\ FR\ inlet}}\right) \times 100 \quad (2)$$

$$\mathrm{CO_2\ purity} = \left(\frac{\mathrm{CO_2\ flowrate\ at\ FR\ outlet}}{\mathrm{Total\ flowrate\ at\ FR\ outlet}}\right) \times 100 \quad (3)$$

Similarly, for the gas leakage during CLR experiments, the syngas recovery is obtained as the ratio between the syngas leaks from the FR to the AR and the total amount of syngas produced in the FR. Syngas purity calculated based on the N_2 leaking from the AR to the FR and the total amount of syngas produced in the FR.

The following reactions are involved in the CLR process. It is noted that R1 and R2 occur primarily as combinations of R3-R6.

Fuel reactor:

$$CH_4 + NiO \leftrightarrow CO + 2H_2 + Ni \quad R1$$

$$CH_4 + 4NiO \leftrightarrow CO_2 + 2H_2O + 4Ni \quad R2$$

$$CH_4 + H_2O \leftrightarrow CO + 3H_2 \quad R3$$

$$CO + H_2O \leftrightarrow CO_2 + H_2 \quad R4$$

$$H_2 + NiO \rightarrow Ni + H_2O \quad R5$$

$$CO + NiO \rightarrow Ni + CO_2 \qquad R6$$

Air reactor:

$$O_2 + 2Ni \leftrightarrow 2NiO \qquad R7$$

3. Results and Discussions

The results will be presented and discussed in three parts: 1) Solids circulation, 2) Gas leakage, 3) CLR of methane. Table 3 summarizes the main results of the CLR experimental campaigns which will be disused in the following sections.

Table 3. Summary of the main results of the CLR experimental campaigns.

	Product compositions (vol%)					Fuel Reactor		Air Reactor		Syngas recovery %	Syngas purity %	T-FR (°C)	T-AR (°C)
	CH_4	CO_2	CO	H_2	N_2	CH_4 Conv %	H_2/CO	O_2 Conv %	CO_2 vol %				
Case-3	1.7	29.2	0.4	0.0	68.7	94.7	0.0	28.8	0.43	88.6	90.7	764	800
Case-4	0.8	30.3	5.7	10.5	52.6	97.8	1.83	30.0	0.51	88.9	90.9	760	810
Case-5	0.9	31.1	10.8	22.9	34.4	98.1	2.13	34.3	0.46	91.3	93.0	745	785
Case-6	2.0	31.8	19.7	41.3	5.3	96.3	2.09	33.8	0.38	94.1	95.2	753	793
Case-7	1.5	19.4	14.0	31.2	33.9	95.8	2.22	96.4	0.31	93.9	94.9	746	765
Case-8	3.4	13.9	23.7	51.1	7.9	91.7	2.16	100.0	1.14	81.2	84.1	740	765
Case-9	3.7	19.2	15.3	51.5	10.3	90.3	3.36	23.8	0.61	87.2	89.1	721	753

3.1. Solids circulation

The solids circulation rate is a critical operating variable for the chemical looping reforming process. Estimating the solids circulation rate in a hot, pressurized ICR system is a challenging task because no direct measurement technique is possible. In this study, we follow the indirect approach described in Section 2.4 to define an operating window where solids circulation is sufficient for CLR process.

Fig. 4. shows the profile of CO conversion with time for different N_2 flowrates in the AR. Complete CO conversion was observed for all cases during the first minute of operation before gradually reducing with time as the oxidized oxygen carrier is consumed in absence of an air feed for reoxidation. The test was stopped at a certain level of CO conversion (~20%) to avoid

carbon deposition in the existence of highly reduced oxygen carrier as metallic Ni is well known to catalyze CO decomposition. The case of not feeding N_2 to the AR shows that the oxygen carrier in the fuel reactor can be reduced in about 160 s if no solids circulation takes place. With introducing N_2 to the AS, the time almost doubled, implying successful solids circulation and reduction of all the OC loaded in the reactor. Only minor differences were observed between the three N_2 feed rates investigated, implying that the range of 70-90 Nl/min feed to the AR is safe for achieving good solids circulation in the reactor.

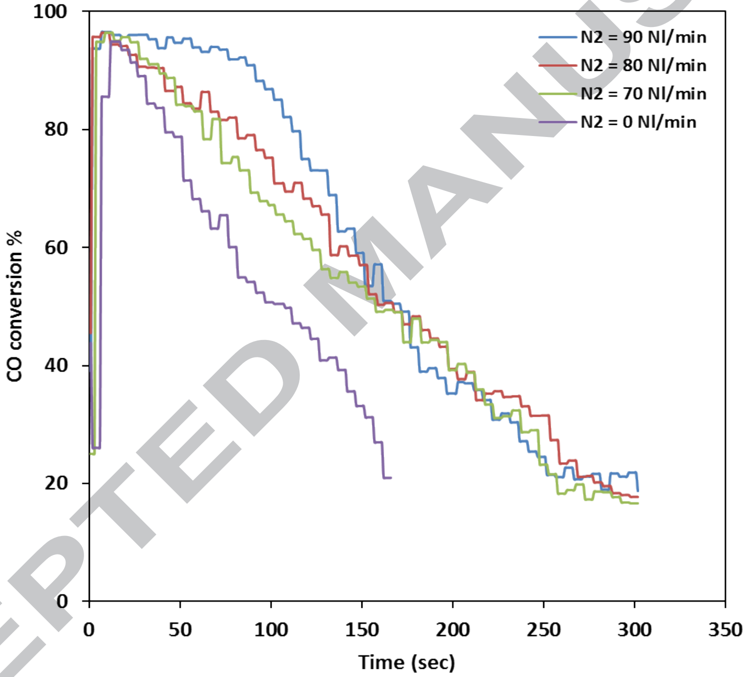

Fig. 4. Temporal evolution of CO conversion for different N_2 flowrates in the AR, Case-1.

3.2. Gas leakage

Gas leakage between FR and AR is undesirable in CLR process because it lowers syngas recovery and purity. In the pseudo-2D ICR cold study, we have shown that gas leakage can be controlled by ensuring that the gas outflow is equivalent to the gas inflow in each section [33]. In the non-reactive gas leakage study described in Section 2.4, analysis from the outlets of the FR and AR shows that 1.7 vol% of the air feed bypassed to the FR and 9 vol% of CO_2 feed bypassed to the AR. This corresponds to 91 % CO_2 recovery and purity.

In a similar ICR concept, Kronberger et, al. [40] carried out a cold flow study of a two compartment fluidized-bed reactor with different slots design connecting the two beds. A slot design with a height of 1.2 mm and an 8 mm wide was found to be the best in achieving a minimum gas leakage. This design has also the possibility of fluidization with inert gas below the slot, which is further reduce the gas leakage. Subsequent studies for CLC and CLR process in a 300 W unit showed that the leakage from the FR to the AR was about 5% of the added carbon, whereas the leakage flow in the opposite direction was 0-0.2% of the added air [45]. Herguido et, al. [41] also applied ICR concept for hydrogen separation using the steam-iron process. They studied the effect of several parameters on gas leakage and solid circulation. Fluidization velocity in both sections and design of the orifice connected the reactor sections found to be the key parameters for controlling gas leakage and solid circulation rate. An orifice diameter of 0.3 cm was found to be an optimal in achieving sufficient solid circulation rate while minimizing the gas leakage.

All fully reactive CLR tests in the following sections were completed with identical operating conditions (temperature, fluidization velocity and solids loading), so it is expected that similar gas leakage will be observed. It is expected that gas leakage occurs mainly through the top port as this port will not be completely filled with particles due to the small quantity of oxygen carrier used in these tests. A filled port is important to restrict uncontrolled gas slippage between the two reactor sections [33]. The possibility for further decreases in gas leakage will be further investigated in future works with different oxygen carrier loadings and fluidization velocities.

3.3. Chemical looping reforming of methane (excess air)

The ICR unit used in this study was designed to test a number of different chemical looping concepts, hence the equal cross sections of the AR and FR of the reactor (Fig. 2). In CLR, the air requirement is much smaller than in CLC, implying that a feed of pure air to the AR at the high flowrate required to achieve solids circulation will provide excess oxygen. In this case, however, the oxygen transport to the FR was limited by the oxygen carrier circulation rate, not by the amount of oxygen fed to the AR. This allowed the CH_4/O_2 ratio to be controlled by simply varying the degree of fuel dilution, while feeding an excess of air to the AR (cases 3-6 in Table 1). The CH_4/O_2 ratio in the FR controls the tendency towards reforming or combustion. Gas concentration measurements at the AR outlet showed that only about a third of the incoming oxygen (~5.6 Nl/min) was consumed in these cases. This results in CH_4/O_2 ratios of 0.54-0.89 for the four cases investigated in this section.

Fig. 5 and Fig. 6 show the results from this experimental campaign. Case-3 showed near complete combustion of CH_4 to CO_2 and H_2O, which implies an excess of NiO in the fuel reactor (R2). A minor amount of CO was also detected, although H_2 is completely consumed due to its very high reactivity with NiO. This may be expected given that the CH_4/O_2 ratio is close to the stoichiometric ratio of 0.5 for methane combustion. Increasing the methane flowrate from 3 Nl/min to 5 Nl/min increases the CH_4/O_2 ratio and therefore shifts the reaction further towards reforming instead of combustion, producing more H_2 and CO (R1). For case 5 and 6, an H_2/CO ratio of 2 was obtained, which is desirable for the Fischer-Tropsch process [46].

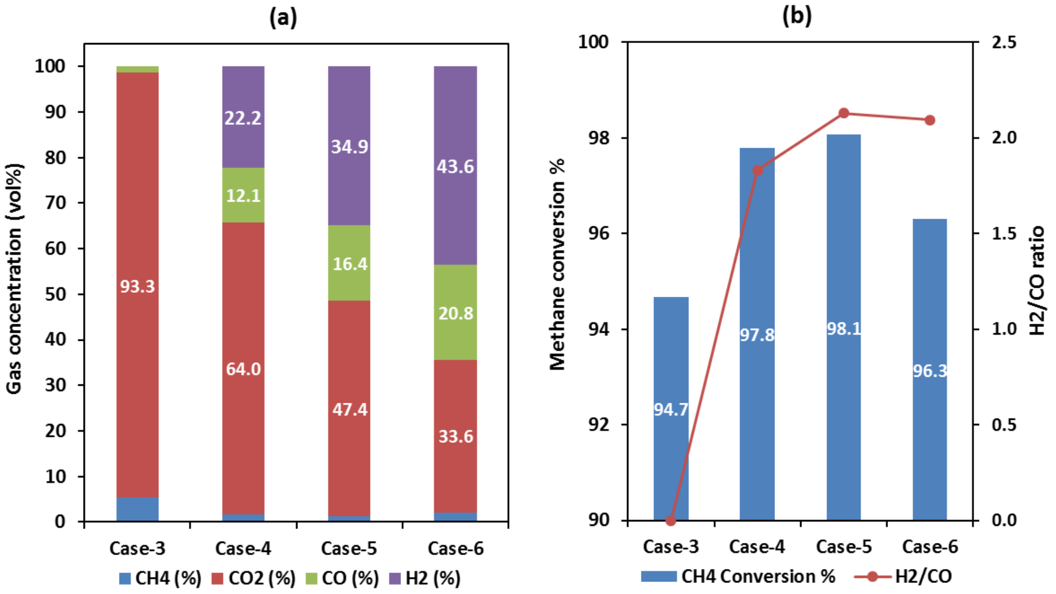

Fig. 5. Products distribution (a) and methane conversion and H_2/CO ratio (b) for cases 3-6.

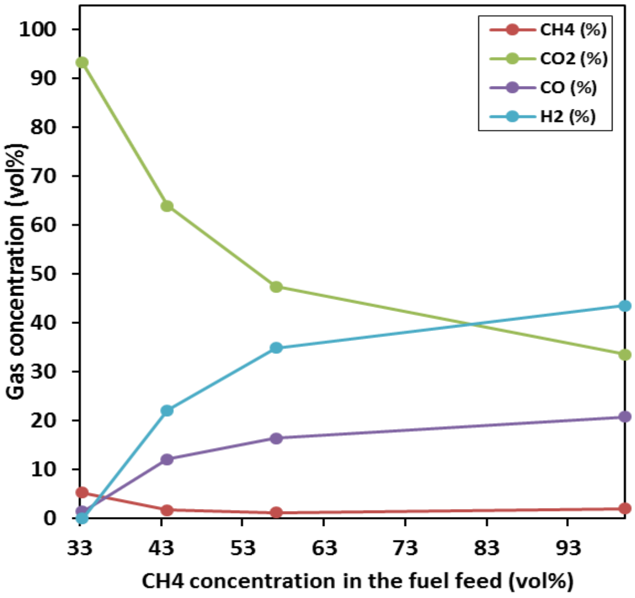

Fig. 6. Effects of methane concentration on the products compositions.

Fig. 5b shows the methane conversion level for cases 3-6. The first observation is that methane conversion is higher than 94% in all cases. This is testament to the extremely high reactivity of the NiO oxygen carrier used in this study. It is worthwhile to keep in mind that the bed height in the FR is only 10 cm and that the gas is injected in a relatively concentrated manner, imposing significant bubble-to-emulsion mass transfer limitations. Under similar conditions, a larger reactor will therefore easily achieve complete equilibrium conversion.

The second observation is that maximum methane conversion is reached at intermediate CH_4/O_2 ratios. This trend of methane conversion over NiO is associated with the degree of oxygen carrier reduction and the presence of H_2O and CO_2 in the FR. With a fixed solids circulation rate, increasing the fuel concentration in the FR will affect the OC reduction level and hence its activity and selectivity for methane reactions. A similar trend was revealed by several studies on CLC and CLR [11,47–51]. A study of methane CLC over NiO in a fixed bed reactor observed methane slippage during the first part of the reduction when the particles were fully oxidized, which disappeared as the particles became more reduced, i.e. the content of Ni increased [51]. Thus, at lower CH_4/O_2 ratios, the oxygen carrier was not sufficiently reduced to rapidly catalyze the reforming reaction on free Ni sites, resulting in reaction rate-limited methane conversion. At high CH_4/O_2 ratios, on the other hand, the lower fraction of CH_4 combustion produced a lower concentration of H_2O and CO_2 in the reactor, results in equilibrium limitations for the methane reforming reactions. When only CH_4 is fed to the reactor, a large portion of this fuel must be combusted to H_2O and CO_2 to promote the Ni-catalyzed steam and dry reforming reactions, otherwise the degree of methane conversion will be thermodynamically limited.

Autothermal operation of ICR was investigated for these cases. Case 5 and 6 achieved autothermal operation successfully. Fig. 7. shows the temperature profile for case 5: the temperature was constant in both sections for about 20 min of continuous operation without external heating. The temperature difference was 40°C between the two sections. Circulation of the OC and the heat transfer through the wall separating the two sections were the only source of heat for the reforming reactions during this investigation.

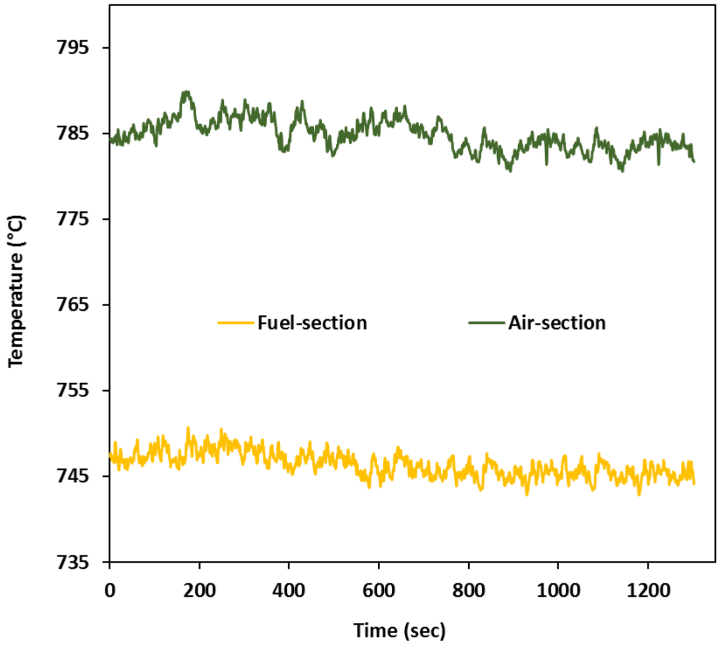

Fig. 7. Temperature of FR and AR during autothermal chemical looping reforming of methane (case-5).

3.4. Chemical looping reforming of methane (diluted air)

In a second series of experiments, the oxygen supply to the AR was limited by N_2 dilution (case 7 and 8). In both cases, almost complete oxygen conversion was achieved (Table 3), which represents more realistic CLR behavior where the oxygen carrier circulation rate is not the limiting factor in oxygen transport between reactor sections as was the case in the previous section. Consequently, the oxygen added to the AR in cases 7 and 8 is not sufficient to reoxidize the OC completely. The OC flowing from the AR to the FR is therefore in a less oxidized form, leading to higher reforming activity and, assuming a constant solids circulation rate, a lower flow of oxidized oxygen carrier to the FR.

The comparison between case 5 and case 7 was designed to achieve roughly the same CH_4/O_2 ratio in the FR. However, a significant difference in FR outlet gas composition and methane conversion is observed between these two cases because of the aforementioned factors. The increased presence of Ni and the lower presence of NiO in case 7 caused a higher fraction of H_2 and CO, but lower methane conversion relative to case 5 (Fig. 8).

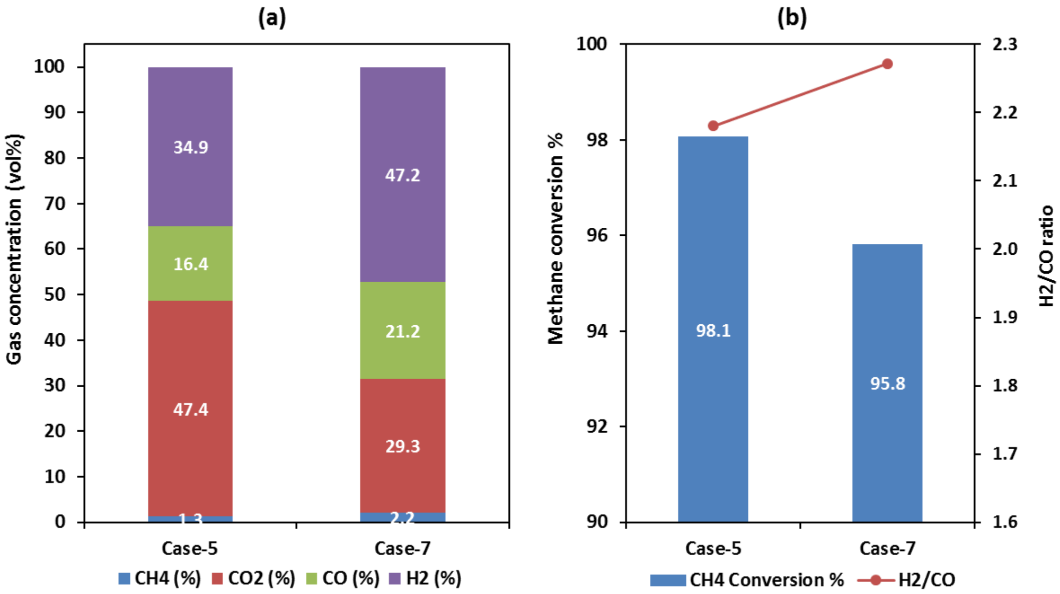

Fig. 8. Products distribution (a) and methane conversion and H_2/CO ratio (b) for cases 5 and 7.

Case 8 was designed to achieve a substantially higher CH_4/O_2 ratio than case 6 (Fig. 9). Naturally, this further increased the degree of reduction of the oxygen carrier entering the FR from the AR, leading to a greater shift towards H_2 and CO as well as a lower degree of methane conversion (thermodynamically limited due to the relatively low fraction of CH_4 combusted to H_2O and CO_2).

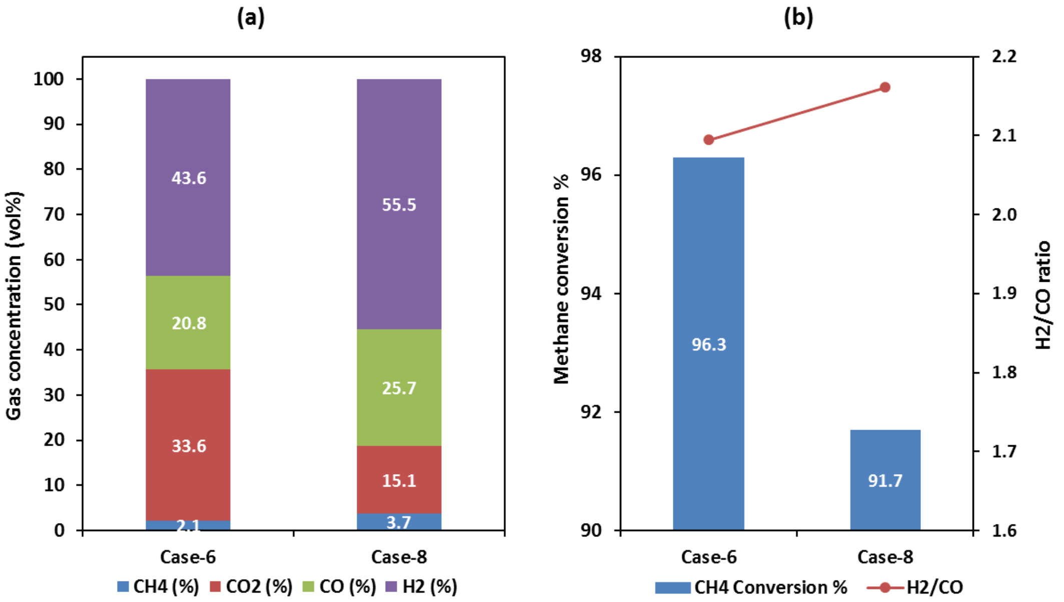

Fig. 9. Products distribution (a) and methane conversion and H_2/CO ratio (b) for cases 6 and 8.

Further insight is provided by comparing the observed reactor performance to equilibrium calculations. These results were obtained using the equilibrium module of the HSC chemistry software 9.2, which is based on the method of minimization of the Gibbs free energy [52]. Fig. 10 shows the comparison of the gaseous products obtained in case-5 to case-8 and the equilibrium compositions as a function of the CH_4/O_2 ratio for a reaction temperature of 746°C, and pressure of 1.7 bara. The temperature selected as an average temperature between case-5, case-6, case-7 and case-8, whereas the CH_4/O_2 ratio for these cases are 0.69, 0.88, 0.79 and 1.19, respectively.

Despite some scatter in the experimental results, it follows the same trend as the equilibrium calculations. The equilibrium composition of methane increases with increasing CH_4/O_2 ratio, which validates the drop of methane conversion in case-7 and case-8 compared to case-5 and case-6, respectively. Equilibrium is not reached mainly because of CH_4 slippage. This is attributed to a reaction rate limitation caused by the short bed height in the FR and the concentrated gas injection mechanism that limits gas-solid contact. Furthermore, the experimental H_2 and CO concentrations are lower than the equilibrium calculations because these gases react more rapidly than CH_4 with NiO. For instance, Wassie et al. [28] showed that CH_4 fed to a bed of NiO results in substantial fuel slippage, whereas a feed of H_2 results in complete fuel conversion. NiO enters from the top of the FR, while most reforming occurs over the reduced OC at the bottom of the FR. Therefore, NiO is primarily reduced to Ni in the upper regions of the bed by H_2 and CO resulting from steam-methane reforming in the lower regions of the bed. If the FR was perfectly mixed, the experimental observations would be even closer to the equilibrium calculations.

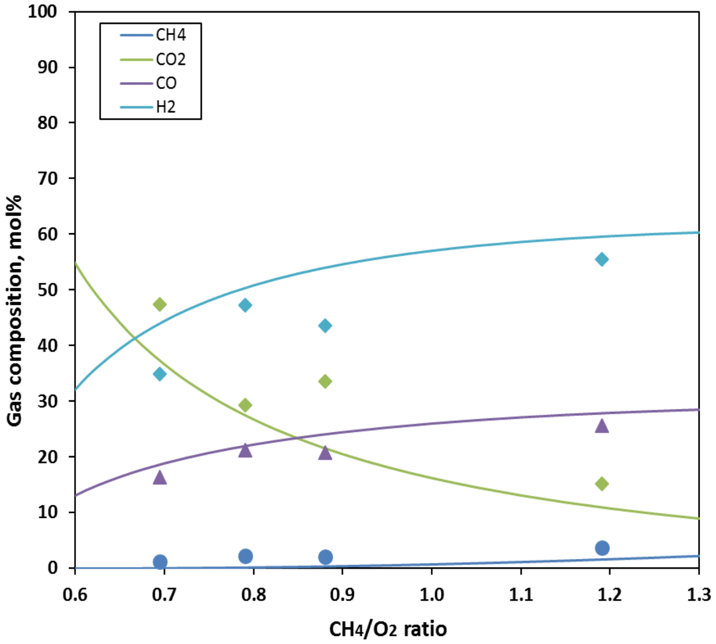

Fig. 10. Dry gas compositions according to cases (5)-(8) compared to thermodynamic equilibrium for CLR of methane at 746°C and 1.7 bara.

3.5. Chemical looping reforming of methane (steam addition)

Partial oxidation of methane typically produces syngas with H_2/CO ratio of 2, as observed in the previous cases (case 4-8). Addition of steam with methane into the FR is the most suitable approach to increase the H_2 content in the syngas and prevent carbon formation. Steam boosts the catalytic methane reforming over metallic Ni (R3), which increases the H_2/CO ratio in the syngas produced. This process would be the most suitable one for H_2 production. Furthermore, additional steam will alleviate the equilibrium limitations on methane conversion observed when only CH_4 is fed to the reactor at a high CH_4/O_2 ratio (e.g. case 8).

In the current study, addition of steam with the fuel feed was investigated (case-9). An S/C ratio of 1.33 was chosen to keep the total flowrate constant and hence compare all results under similar hydrodynamic conditions. As shown in Fig. 10, addition of steam enhances the methane reforming reactions, producing more H_2 and less CO_2, 57 vol% H_2 (dry basis) was produced compared to 35 vol% for the dry fuel feed (case-5). The H_2/CO ratio increases from 2.1 to 3.4 upon steam co-feeding.

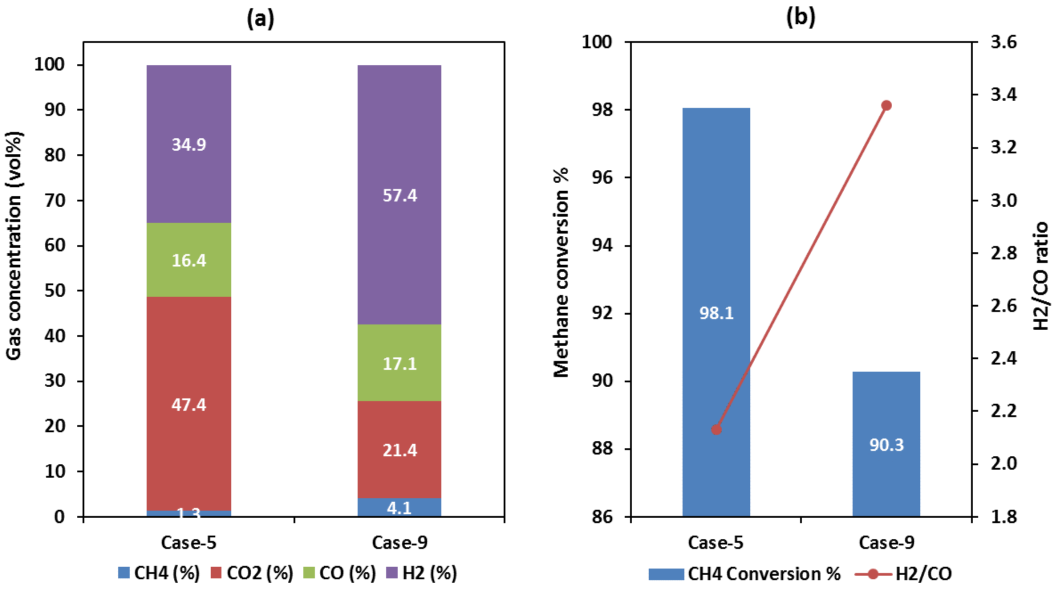

Fig. 11. Products distribution (a), Methane conversion and H_2/CO ratio (b). comparing case 5 and 9.

Surprisingly, methane conversion dropped to 90% compared to 98% in case-5. Methane conversion is expected to increase with steam addition due to a favorable shift in the equilibrium of the steam reforming reaction (R3). The FR temperature is lower by 24°C in case-9 compared to case-5 (see Table 3) due to the strong endothermicity of the steam reforming reaction.

Thermodynamic calculations showed a drop of less than 1.0% of methane conversion due to the lower reactor temperature in case-9. The lower reactor temperature will also lead to lower reaction rates, limiting methane conversion further below the equilibrium prediction. Another contributing factor could be the difference of the oxidation/reduction state of the oxygen carrier in the FR for case-5 and case-9. In case-9, the oxygen consumption in the AR was lower compared to case-5 (as in Table 3) since part of methane in the FR is involved in the steam reforming R3. This led to lower solids conversion and hence a lower Ni/NiO ratio in the FR limiting the catalytic activity of the oxygen carrier. This phenomenon has been revealed by the current study in case-3 to case-6, also in earlier studies [11,47–51,53,54].

Overall, the results presented in this study are comparable with findings reported by other CLR experimental studies. Diego et al [12,55] conducted CLR operation in a 900 W dual circulating fluidized bed reactor using methane as fuel and a total of 1.5 kg of a nickel based oxygen carrier. They reported a high methane conversion over a wide range of operating conditions. The solid circulation rate (NiO/CH_4 molar ratio) was the most influential variable on the products distribution. Autothermal operation could be achieved with a NiO/CH_4 molar ratio of 1.25, and the product composition at this condition was 65 vol.% H_2, 25 vol.% CO, 9 vol.% CO_2, and 1-1.5 vol.% CH_4. A maximum of 25% steam added with methane slightly changed the products distribution and reduced the carbon deposition. Comparable results were also observed by Rydèn et.al [6] in a 300 W two compartment fluidized beds reactor.

3.6. Gas leakage during CLR operation

The gas leakage between the two sections is a critical parameter in ICR, and should be minimized to maximize syngas recovery and purity. If there is a leakage from the FR to the AR, the syngas recovery will decrease since part of the produced syngas will be lost through the AR.

Gas leakage into the other direction will cause the syngas stream to be diluted with nitrogen reducing the syngas purity. During the CLR tests, the air leakage from the AR to the FR can be estimated based on the N_2 concentration in the FR exhaust gas. The O_2 leaked from the AR to the FR will either react with the oxygen carrier or combust part of the syngas. The leakage of the syngas from the FR to the AR can be estimated from the CO_2 concentration at the AR outlet. A minor amount of CO_2 could also form in the AR as a result of carbon deposition in the FR. Table 3 shows the calculated syngas recovery and purity in each case. One can observe that the syngas recovery and purity is in the range of 81% to 95%. The values are rather scattered, but in a similar range compared to the non-reactive leakage test, which showed a CO_2 recovery and purity of 91%. This similarity is expected, given that variations in the solids circulation were minimized by aiming for constant fluidization velocities in both sections (under the assumption that all CH_4 is converted) and constant solids loading in all cases. The deviation occurs in the CLR tests mainly due to reduction of the air flowrate after O_2 consumption in the AR, the incomplete methane conversion in the FR, and the variation in the gas composition (and therefore the gas density and viscosity) in the FR.

Case-8 showed the highest CO_2 concentration in the AR (Table 3) compared to other cases, this could be due to carbon deposition in the FR, which led to extra CO_2 release when the deposited carbon is oxidized in the AR. In this specific case, insufficient oxygen was supplied to the AR to fully oxidize the oxygen carrier (no O_2 was observed in the AR outlet), so the OC flowing from the AR to the FR was in less oxidized form. This will result in a higher Ni/NiO ratio compared to other cases, which promotes methane decomposition to C and H_2 over the Ni catalyst. Therefore, the calculated syngas recovery in this case should be higher than the reported value (81%) after excluding part of the CO_2 that released due to carbon combustion.

4. Summary and conclusion

This study has successfully demonstrated chemical looping reforming (CLR) of methane in a novel internally circulating reactor (ICR). The reactor was especially designed to simplify scale up of the conventional dual circulating fluidized bed chemical looping configuration, especially under pressurized conditions. In ICR, the functionality of two reactors, two cyclones and two loop seals is packaged into a single unit, which can be designed and operated in a single pressure shell.

The large degree of process simplification offered by the ICR concept comes with a trade-off in the form of increased gas leakage between the two reactor sections. In this study, CO_2 leakage to the air reactor and dilution of the syngas by N_2 leaking from the air reactor was about 9% on average, although substantial improvements are expected as more operating experience is gained.

CLR operation was conducted in three separate studies. Firstly, air was fed in excess to the AR. It was found that oxygen transport to the FR was limited by the oxygen carrier circulation rate, allowing for a modification of the CH_4/O_2 ratio by only changing the amount of methane feed to the FR. The reactor behaved largely as expected, showing almost no syngas production when the CH_4/O_2 ratio was close to 0.5 (stoichiometric ratio for combustion), but steadily increasing syngas production when the CH_4/O_2 ratio was increased. Low CH_4/O_2 ratios experienced reaction rate limitations and high CH_4/O_2 ratios experienced thermodynamic limitations, resulting in an optimal methane conversion of 98% at intermediate CH_4/O_2 ratios.

Subsequently, the O_2 feed to the AR was reduced so that the oxygen carrier circulation rate was no longer the limiting factor in oxygen transport to the FR. As expected, this led to higher CH_4/O_2 ratios, resulting in more reforming activity, but also lower, thermodynamically limited methane conversions. Finally, a case with additional steam feed to the FR was completed to demonstrate how the H_2/CO ratio of the produced syngas could be increased from 2 in the cases with only methane feed to higher values that are more applicable to hydrogen production.

Autothermal operation could be achieved in some of the cases, further illustrating the functionality of the ICR concept. Overall, this first concept demonstration study was successful and further study of the ICR concept applied to different chemical looping concepts over a wider range of temperatures and pressures is strongly recommended.

Acknowledgment

The authors would like to acknowledge the financial support of the Research Council of Norway under the CLIMIT program (project number: 255462). The technical support from Mr. Martin Bustadmo and Mr. Paul Svendsen is highly appreciated.

Abbreviations

ICR	Internally circulating reactor
CLR	Chemical looping reforming
CLC	Chemical looping combustion
SMR	Steam methane reforming
AR	Air reactor
FR	Fuel reactor
OC	Oxygen carrier

References

[1] J.R. Rostrup-Nielsen, Syngas in perspective, Catal. Today. 71 (2002) 243–247.
[2] P. Nikolaidis, A. Poullikkas, A comparative overview of hydrogen production processes, Renew. Sustain. Energy Rev. 67 (2017) 597–611.
[3] I. Dincer, C. Acar, Review and evaluation of hydrogen production methods for better sustainability, Int. J. Hydrogen Energy. 40 (2015) 11094–11111.

[4] J.D. Holladay, J. Hu, D.L. King, Y. Wang, An overview of hydrogen production technologies, Catal. Today. 139 (2009) 244–260.

[5] M. Rydén, A. Lyngfelt, Using steam reforming to produce hydrogen with carbon dioxide capture by chemical-looping combustion, Int. J. Hydrogen Energy. 31 (2006) 1271–1283.

[6] M. Ryden, A. Lyngfelt, T. Mattisson, Synthesis gas generation by chemical-looping reforming in a continuously operating laboratory reactor, Fuel. 85 (2006) 1631–1641.

[7] Y. Khojasteh Salkuyeh, B.A. Saville, H.L. MacLean, Techno-economic analysis and life cycle assessment of hydrogen production from natural gas using current and emerging technologies, Int. J. Hydrogen Energy. 42 (2017) 18894–18909.

[8] T. Pröll, J. Bolhàr-Nordenkampf, P. Kolbitsch, H. Hofbauer, Syngas and a separate nitrogen/argon stream via chemical looping reforming – A 140 kW pilot plant study, Fuel. 89 (2010) 1249–1256.

[9] M. Ortiz, L.F. de Diego, A. Abad, F. García-Labiano, P. Gayá, J. Adá Nez, P. Gayán, J. Adánez, Hydrogen production by auto-thermal chemical-looping reforming in a pressurized fluidized bed reactor using Ni-based oxygen carriers, Int. J. Hydrogen Energy. 35 (2010) 151–160.

[10] M. Rydén, A. Lyngfelt, T. Mattisson, Chemical-looping combustion and chemical-looping reforming in a circulating fluidized-bed reactor using Ni-based oxygen carriers, Energy and Fuels. 22 (2008) 2585–2597.

[11] M. Rydén, M. Johansson, A. Lyngfelt, T. Mattisson, NiO supported on Mg–ZrO2 as oxygen carrier for chemical-looping combustion and chemical-looping reforming, Energy Environ. Sci. 2 (2009) 970.

[12] L.F. De Diego, M. Ortiz, F. García-Labiano, J. Adánez, A. Abad, P. Gayán, Hydrogen production by chemical-looping reforming in a circulating fluidized bed reactor using Ni-based oxygen carriers, J. Power Sources. 192 (2009) 27–34.

[13] P. Moldenhauer, M. Rydén, T. Mattisson, A. Lyngfelt, Chemical-looping combustion and chemical-looping reforming of kerosene in a circulating fluidized-bed 300 W laboratory reactor, Int. J. Greenh. Gas Control. 9 (2012) 1–9.

[14] F. García-Labiano, E. García-Díez, L.F. De Diego, A. Serrano, A. Abad, P. Gayán, J. Adánez, J.A.C. Ruíz, Syngas/H2 production from bioethanol in a continuous chemical-looping reforming prototype, Fuel Process. Technol. 137 (2015) 24–30.

[15] B. Dou, Y. Song, C. Wang, H. Chen, M. Yang, Y. Xu, Hydrogen production by enhanced-sorption chemical looping steam reforming of glycerol in moving-bed reactors, (2014).

[16] H. Ge, W. Guo, L. Shen, T. Song, J. Xiao, Biomass gasification using chemical looping in a 25 kW th reactor with natural hematite as oxygen carrier, Chem. Eng. J. 286 (2016) 174–183.

[17] H. Ge, W. Guo, L. Shen, T. Song, J. Xiao, Experimental investigation on biomass gasification using chemical looping in a batch reactor and a continuous dual reactor, (2016).

[18] M. Luo, Y. Yi, S. Wang, Z. Wang, M. Du, J. Pan, Q. Wang, Review of hydrogen production using chemical-looping technology, Renew. Sustain. Energy Rev. 81 (2018) 3186–3214.

[19] J. Adanez, A. Abad, F. Garcia-Labiano, P. Gayan, L.F. de Diego, Progress in Chemical-Looping Combustion and Reforming technologies, Prog. Energy Combust. Sci. 38 (2012) 215–282.

[20] W. Wang, Y. Cao, A combined thermodynamic and experimental study on chemical-looping ethanol reforming with carbon dioxide capture for hydrogen generation, Int. J.

Energy Res. 37 (2013) 25–34.
[21] S.M. Nazir, O. Bolland, S. Amini, Full Plant Scale Analysis of Natural Gas Fired Power Plants with Pre-Combustion CO2 Capture and Chemical Looping Reforming (CLR), Energy Procedia. 114 (2017) 2146–2155.
[22] S. Wang, G. Wang, F. Jiang, M. Luo, H. Li, Chemical looping combustion of coke oven gas by using Fe2O3/CuO with MgAl2O4 as oxygen carrier, Energy Environ. Sci. 3 (2010) 1353–1360.
[23] T. Song, T. Shen, L. Shen, J. Xiao, H. Gu, S. Zhang, Evaluation of hematite oxygen carrier in chemical-looping combustion of coal, Fuel. 104 (2013) 244–252.
[24] A. Zaabout, S. Cloete, S.T. Johansen, M. Van, S. Annaland, F. Gallucci, S. Amini, Experimental Demonstration of a Novel Gas Switching Combustion Reactor for Power Production with Integrated CO2 Capture, Ind. Eng. Chem. Res. 52 (2013) 14241−14250.
[25] S. Noorman, M.V.S. Annaland, H. Kuipers, Packed Bed Reactor Technology for Chemical-Looping Combustion, Ind. Eng. Chem. Res. 46 (2007) 4212–4220.
[26] H.P. Hamers, F. Gallucci, G. Williams, M. van Sint Annaland, Experimental demonstration of CLC and the pressure effect in packed bed reactors using NiO/CaAl2O4 as oxygen carrier, Fuel. 159 (2015) 828–836.
[27] A. Zaabout, S. Cloete, S. Amini, Autothermal operation of a pressurized Gas Switching Combustion with ilmenite ore, Int. J. Greenh. Gas Control. 63 (2017) 175–183.
[28] S.A. Wassie, F. Gallucci, A. Zaabout, S. Cloete, S. Amini, M. Van, S. Annaland, Hydrogen production with integrated CO2 capture in a novel gas switching reforming reactor: Proof-of-concept, Int. J. Hydrogen Energy. 42 (2017) 14367–14379.
[29] S. Cloete, F. Gallucci, M. van Sint Annaland, S. Amini, Gas Switching as a Practical Alternative for Scaleup of Chemical Looping Combustion, Energy Technol. 4 (2016) 1286–1298.
[30] A. Tong, L. Zeng, M. V. Kathe, D. Sridhar, L.-S. Fan, Application of the Moving-Bed Chemical Looping Process for High Methane Conversion, Energy & Fuels. 27 (2013) 4119–4128.
[31] S.F. Håkonsen, R. Blom, Chemical Looping Combustion in a Rotating Bed Reactor – Finding Optimal Process Conditions for Prototype Reactor, Environ. Sci. Technol. 45 (2011) 9619–9626.
[32] Z. Zhao, T. Chen, A.F. Ghoniem, Rotary Bed Reactor for Chemical-Looping Combustion with Carbon Capture. Part 1: Reactor Design and Model Development, Energy Fuels. 27 (2013) 327−343.
[33] A. Zaabout, S. Cloete, S. Amini, Innovative Internally Circulating Reactor Concept for Chemical Looping-Based CO2 Capture Processes: Hydrodynamic Investigation, Chem. Eng. Technol. 39 (2016) 1413–1424.
[34] S. Cloete, A. Zaabout, S. Amini, The Internally Circulating Reactor (ICR) Concept Applied to Pressurized Chemical Looping Processes, Energy Procedia. 114 (2017) 446–457.
[35] Y.-0 Y.-O. Chong, D.J.J. Nicklin, P.J.J. Tait, Solids exchange between adjacent fluid beds without gas mixing, Powder Technol. 47 (1986) 151–156.
[36] A. Abad, T. Mattisson, A. Lyngfelt, M. Ryden, Chemical-looping combustion in a 300W continuously operating reactor system using a manganese-based oxygen carrier, Fuel. 85 (2006) 1174–1185.
[37] T. Mattisson, F. García-Labiano, B. Kronberger, A. Lyngfelt, J. Adánez, H. Hofbauer, Chemical-looping combustion using syngas as fuel, Int. J. Greenh. Gas Control. 1 (2007)

158–169.

[38] E. Johansson, T. Mattisson, A. Lyngfelt, H. Thunman, Combustion of Syngas and Natural Gas in a 300 W Chemical-Looping Combustor, Chem. Eng. Res. Des. 84 (2006) 819–827.

[39] E. Johansson, T. Mattisson, A. Lyngfelt, H. Thunman, A 300 W laboratory reactor system for chemical-looping combustion with particle circulation, Fuel. 85 (3AD) 1428–1438.

[40] B. Kronberger, E. Johansson, G. Löffler, T. Mattisson, A. Lyngfelt, H. Hofbauer, A Two-Compartment Fluidized Bed Reactor for CO 2 Capture by Chemical-Looping Combustion, Chem. Eng. Technol. 27 (2004) 1318–1326.

[41] E. Jerndal, T. Mattisson, I. Thijs, F. Snijkers, A. Lyngfelt, NiO particles with Ca and Mg based additives produced by spray- drying as oxygen carriers for chemical-looping combustion, Energy Procedia. 1 (2009) 479–486.

[42] J. Bolhàr-Nordenkampf, T. Pröll, P. Kolbitsch, H. Hofbauer, Performance of a NiO-based oxygen carrier for chemical looping combustion and reforming in a 120 kW unit, Energy Procedia. 1 (2009) 19–25.

[43] T. Mattisson, J. Adanez, T. Proell, R. Kuusik, C. Beal, J. Assinkf, F. Snijkers, A. Lyngfelt, Chemical-looping Combustion CO2 Ready Gas Power, Energy Procedia. 1 (2009) 1557–1564.

[44] C. Linderholm, Thesis for the degree of doctor of philosophy, CO2 Capture using Chemical-Looping Combustion-Operational Experience with Gaseous and Solid Fuels, 2011.

[45] J. Herguido, J.A. Peña, E. Carazo, Experimental assessment of hydrogen separation from H2/CH4 mixtures by the "steam-iron process" in an interconnected circulating fluidized bed reactor, Int. J. Hydrogen Energy. 39 (2014) 14050–14060.

[46] A.Y. Khodakov, W. Chu, P. Fongarland, Advances in the Development of Novel Cobalt Fischer-Tropsch Catalysts for Synthesis of Long-Chain Hydrocarbons and Clean Fuels, Chem. Rev. 107 (2007) 1692–1744.

[47] Q. Zafar, T. Mattisson, R. Gevert, B. Gevert, Integrated Hydrogen and Power Production with CO2 Capture Using Chemical-Looping Reformings Redox Reactivity of Particles of CuO, Mn2O3 , NiO, and Fe2O3 Using SiO2 as a Support, Ind. Eng. Chem. Res. 44 (2005) 3485–3496.

[48] D. Kang, M. Lee, H.S. Lim, J.W. Lee, Chemical looping partial oxidation of methane with CO2 utilization on the ceria-enhanced mesoporous Fe2O3 oxygen carrier, Fuel. 215 (2018) 787–798.

[49] D. Kang, H.S. Lim, M. Lee, J.W. Lee, J.W. Lee, Syngas production on a Ni-enhanced Fe2O3/Al2O3 oxygen carrier via chemical looping partial oxidation with dry reforming of methane, Appl. Energy. 211 (2018) 174–186.

[50] M. Ortiz, L.F. de Diego, A. Abad, F. García-Labiano, P. Gayán, J. Adánez, Catalytic Activity of Ni-Based Oxygen-Carriers for Steam Methane Reforming in Chemical-Looping Processes, Energy & Fuels. 26 (2012) 791–800.

[51] T. Mattisson, M. Johansson, A. Lyngfelt, The use of NiO as an oxygen carrier in chemical-looping combustion, Fuel. 85 (2006) 736–747.

[52] Outotec HSC Chemistry Software 9.2, Equilibrium Compositions Module. https://www.outotec.com/products/digital-solutions/hsc-chemistry

[53] M. Johansson, T. Mattisson, A. Lyngfelt, A. Abad, Using continuous and pulse experiments to compare two promising nickel-based oxygen carriers for use in chemical-looping technologies, (2007).

[54] J.-I. Baek, J.-W. Kim, J.B. Lee, T.H. Eom, J. Ryu, C.K. Ryu, J. Yi, Effects of Support on the Performance of NiO-Based Oxygen Carriers, Oil Gas Sci. Technol. – Rev. IFP Energies Nouvelles. 66 (2011) 223–234.
[55] L.F. de Diego, M. Ortiz, F. García-Labiano, J. Adánez, A. Abad, P. Gayán, Synthesis gas generation by chemical-looping reforming using a Ni-based oxygen carrier, Energy Procedia. 1 (2009) 3–10.

Internally circulating fluidized-bed reactor for syngas production using chemical looping reforming

Mogahid Osman[1], Abdelghafour Zaabout[2], Schalk Cloete[2], Shahriar Amini[1,2*]

[1]Norwegian University of Science and Technology, [2]SINTEF Industry

Trondheim, Norway

HIGHLIGHTS

- Internally circulating reactor (ICR) was proposed and applied for CLR process.
- The ICR is designed to simplify the operation and scale-up of chemical looping processes.
- Sufficient solids circulation rate and low gas leakage was attained.
- High conversion of methane to syngas was achieved.
- Autothermal CLR operation using ICR was demonstrated.